Mediterranean Marine Science

Vol 18, No 2 (2017)

Submarine vortices derived from natural gas hydrate conversion: a mechanism for ocean mixing

A. BARNARD, M. D. MAX, L. GUALDESI

doi: 10.12681/mms.1640

Research Article

Mediterranean Marine Science
Indexed in WoS (Web of Science, ISI Thomson) and SCOPUS
The journal is available on line at http://www.medit-mar-sc.net
DOI: http://dx.doi.org/10.12681/mms.1640

Submarine vortices derived from natural gas hydrate conversion: a mechanism for ocean mixing

A. BARNARD[1], M. D. MAX[2] AND L. GUALDESI[3]

[1] Department of Natural Sciences, University of Houston Downtown, Houston, TX 77002, USA
[2] Department of Geology, University College Dublin, Belfield, Dublin 4, Ireland
[3] Lavimar, Via Delle Cinque Terre, 28, 119123 La Spezia, Italy

Corresponding author: abarnard2@uh.edu

Handling Editor: Vasilios Likousis

Received: 7 January 2016; Accepted: 6 April 2017; Published on line: 12 July 2017

Abstract

We propose that the source water for some abyssal undular vortices cored by cool, low-salinity water identified at depths in excess of 2,500 m in the deepwater region of the Eastern Mediterranean Basin may be related to conversion of natural gas hydrate (NGH) in abyssal marine sediments. The conditions for extensive formation of NGH in the gas hydrate stability zones (GHSZ) of the upper seafloor sediments existed in this region during previous glacial episodes when colder water supported a thicker GHSZ. Seafloor warming during the most recent interglacial caused thinning of the GHSZ at its base and has driven endothermic NGH dissociation that would have released large volumes of low-salinity water and gas that would tend to pond below the base GHSZ. Periodically, trapped low-salinity water and gas would be released into the sea through the overlying sediments. Buoyant low-salinity water masses, supersaturated with gas and locally containing free gas would ascend and introduce a dynamic element into an otherwise generally static environment. As a result of the interaction of the rise of this buoyant plume and Coriolis acceleration the ascending mass would begin to rotate and form a vortex tube in midwater. NGH conversion within the seafloor introduces large coherent masses of low-salinity, lower-temperature water containing a buoyant free gas fraction from near-surface reservoirs into the abyssal depths even where there may only be a weak natural gas petroleum system.

Keywords: Marine geology, hydrates, vortices, bubbles, plumes.

Introduction

An oceanographic survey was conducted in the Ionian abyssal plain region of the Eastern Mediterranean Basin (EMB) as part of site characterizations for a Mediterranean one km^3 Neutrino 'Cosmic Telescope', KM-3Net (Katz, 2006a; Katz & KM3NeT-consortium, 2009; Adrián-Martínez *et al.*, 2014; Adrián-Martínez *et al.*, 2016). This followed on the success of the ANTARES, NEMO (Piattelli & NEMO-collaboration, 2005; Sapienza & collaboration, 2005; Katz, 2006b; Chierici *et al.*, 2012) and NESTOR projects (Aynutdinov *et al.*, 1995; Feder, 2002). As part of the offshore site surveys, temperature sensors and current profilers were installed at depths of 2700 and 3050 m above a ~3350 m flat abyssal plain about 130 km SSE of the SE tip of Sicily (Fig. 1). Current profilers recorded an abyssal current flowing NNW at ~1.9 cm/s at depths exceeding 2,500 m with dipole mesoscale vortices embedded into the flow. Within the current, the profilers measured *in-situ* background temperature values of ~13.87°C at the upper and ~13.84 °C at the lower depths (Rubino *et al.*, 2012). The sensors also measured the anomalous intermittent passage of ~0.05 °C colder water within the interior of the mesoscale vortices. Temperature changes of 0.05 °C are comparable with decadal temperature variation (Rhein *et al.*, 2013). These meso-scale vortices are coherent features spanning over several hundreds of meters vertically and multiple km horizontally. Rubino *et al.* (2012) conclude that there was not enough data for unambiguous identification of the mechanism that produced the vortices. In particular, remote sources for the fresher cooler water could not be identified but they suggested that local, unspecified, causes could have been responsible.

Rotating water masses such as eddies and vortices exist in the oceans over a wide variety of temporal and spatial scales ranging from features driven by global processes such as basin filling gyres, to locally produced turbulence that includes enigmatic features like wave-tube vortices (BBC, 2009), and the relatively high density fluids that create strudel scours. Meso-scale (~10 – ~100 km) vortices, also termed eddies, may travel great distances in the ocean while retaining their coherence. The core of a vortex can deform and twist in geometrically complex ways while retaining the coherence of the internal water mass.

We propose that a large reservoir of natural gas hydrate (NGH) that once existed in the seafloor sediments are responsible for the emission of large volumes of low-salinity water from converted NGH deposits through

the seafloor into the deep oceans. The existence of the hydrate physical-chemical system provides a potential natural mechanism for the delivery of cooler, less saline, water from the seafloor into otherwise generally quiescent deep water masses. NGH present within the EMB seafloor sediments that formed during the previous glacial episode would have dissociated owing to warming of abyssal Mediterranean waters as part of the interglacial equilibration of temperature in the atmosphere-ocean system and the underlying sediment (e.g., Ruppel & Kessler, 2016). Water from converted hydrate is very low-salinity, and even after local mixing with pore water would be considerably less dense and more buoyant than seawater or marine sediment pore water.

NGH conversion provides a mechanism for producing low-salinity water *in-situ* in a deep saline environment completely cut off from any source of fresh surface water provided by the hydrological cycle (e.g., Post *et al.*, 2013). NGH conversion, the process of reducing NGH to its constituent water and natural gas, is naturally accomplished by pressure and/or temperature changes so that the NGH is no longer stable (Max *et al.*, 2006; Max & Johnson, 2016). Conversion of NGH naturally concentrates low-salinity water within sediments that could be released into the water column when buoyancy exceeds hydrostatic and lithostatic retention and thus initiates upwards migration. Once at the seafloor, rising gas and water shape seafloor morphology according to the emission velocity (Roberts *et al.*, 2006).

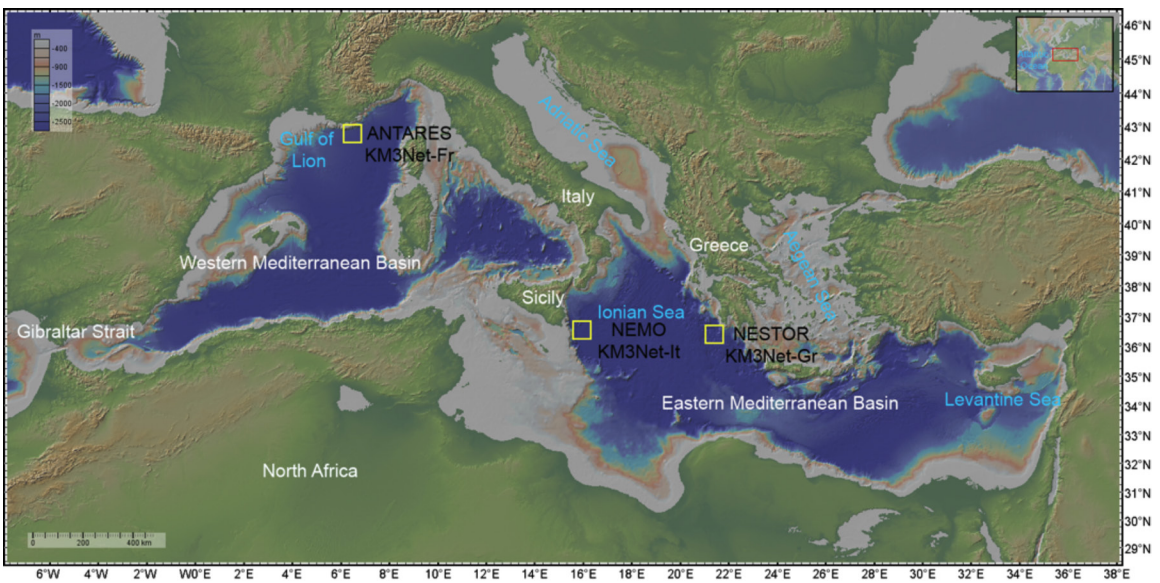

Fig. 1: Mediterranean basin with place names discussed in the text (www.geomapapp.org; Ryan *et al.* (2009).

Mediterranean Oceanic Natural Gas Hydrate

Mean ambient deep water temperatures and salinity are ~13 ˚C and 38.5 $^{0}/_{00}$ respectively, in the vicinity of the vortices (Rubino *et al.*, 2012) which places the NGH stability field at depths below ~1000 m in the water column (Fig. 2). This is about twice as deep than in the cooler global open ocean (Max & Johnson, 2016). Significant NGH deposits also exist beneath the seafloor, and have been identified in the Mediterranean Basin by seismic interpretation and *in-situ* (De Lange & Brumsack, 1998; Aloisi *et al.*, 2000; Loncke *et al.*, 2004; Pierre & Rouchy, 2004; Dählmann, 2005; Lykousis *et al.*, 2009; Perissoratis *et al.*, 2011; Marinakis *et al.*, 2015), and in the Nile fan (Praeg *et al.*, 2011). Global models of NGH thicknesses indicate a 100 – 250 m thick gas hydrate stability zone (GHSZ) in the Mediterranean region (Wood & Jung, 2008) (Fig. 3), which is in agreement with regional models suggesting thicknesses between 200 – 500 m (Praeg *et al.*, 2011). The greatest thicknesses may occur SE of Sicily (Max & Johnson, 2016).

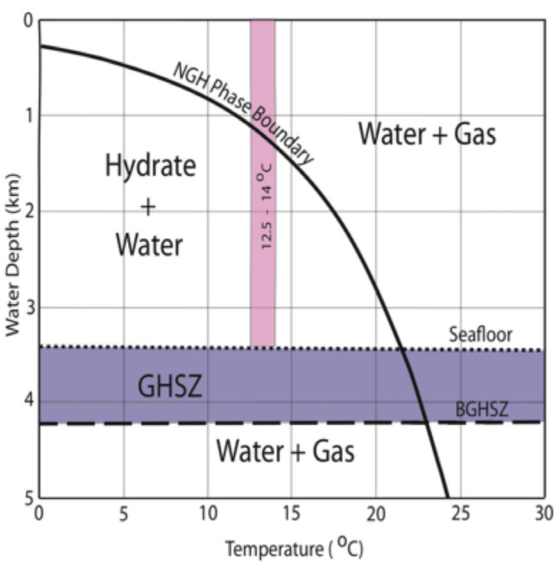

Fig. 2: Generalized phase boundary for methane hydrate in the Mediterranean, redrawn from (Praeg *et al.,* 2011). Increased salinity moves the phase boundary to the left (You *et al.,* 2015).

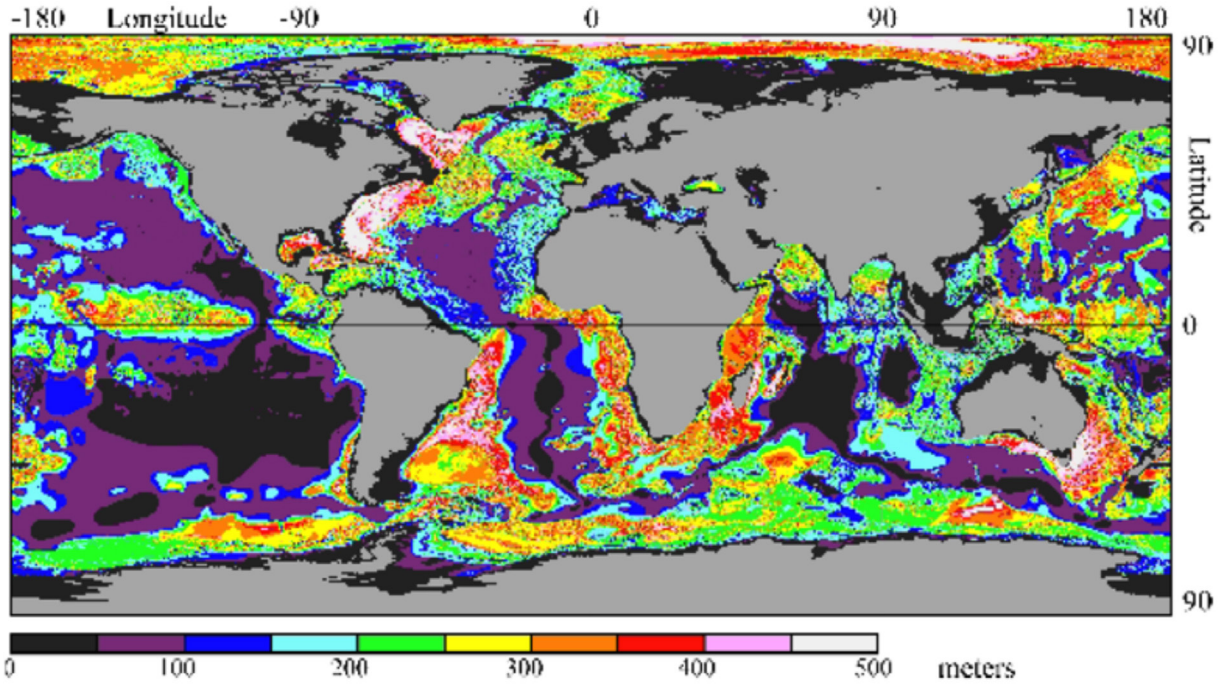

Fig. 3: Global natural gas hydrate stability zone thickness (Wood & Jung, 2008).

Low Salinity Water Fluxes from Natural Gas Hydrate

NGH is a crystalline material formed from water and hydrate-forming gas molecules. In NGH, the predominant gas is methane, but other gases may be present in small amounts. When NGH crystallizes, gas and water molecules combine in an exothermic reaction in which heat is absorbed by its surroundings while brine is rejected (Fig. 4). The salinity of NGH product water mixing with normal pore water has been used to estimate the amount of NGH that had been present prior to dissociation, as shown by drilling on Blake Ridge, Central U.S. East Coast continental slope (Paull *et al.*, 1996; Paull *et al.*, 1998; Holbrook, 2001; Paull & Ussler, 2001; Hesse, 2003). When NGH dissociates in an endothermic reaction, an approximately equal amount of heat per comparable volume of NGH is absorbed from surrounding sediments, as low-salinity water and gas are produced. The product low-salinity water is saturated with gas and free gas that also may remain ponded where it forms in the base GHSZ. Low-salinity water production at virtually all water depths below which NGH is stable is thus possible as an *in-situ* phenomena.

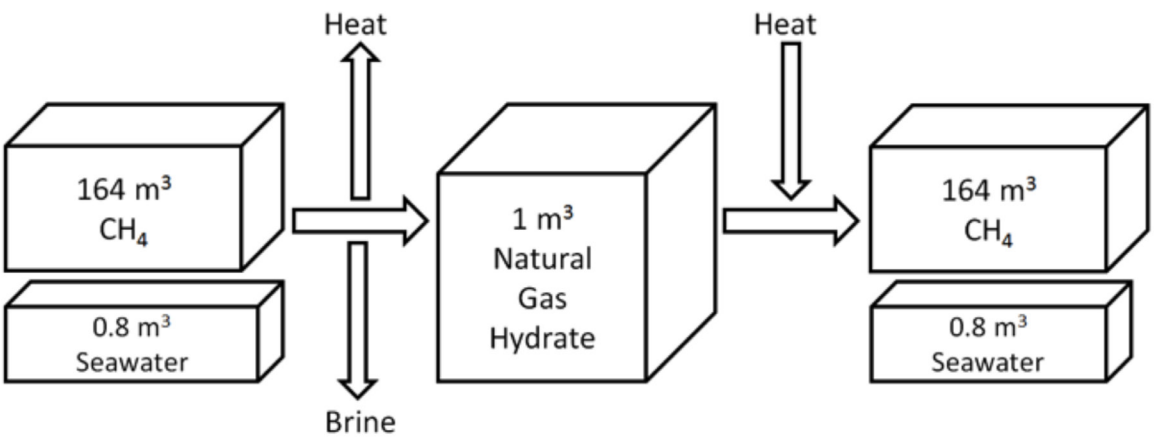

Fig. 4: NGH crystallization - dissociation chemical reaction cycle showing system heat flow and brine rejection. Schematic not to scale.

There are potentially large volumes of low-salinity water held in NGH in deep-sea sediments. Most estimates of NGH are for natural gas in place but considerable low-salinity water would also exist wherever there are large amounts of NGH. Comparison with better-known NGH occurrences allows some estimates of the volumes of low-salinity water that may be released during conversion. Estimates for economic gas-in-place present in global NGH deposits within reservoirs are in excess of ~40,000 TCF (Max & Johnson, 2016). Regionally, NGH deposits in Nankai (JOGMEC, 2013) and Blake Ridge (Dillon & Max, 2001) each contain ~40 TCF gas and ~400 BCF low-salinity water, whereas Walker Ridge houses ~750 BCF gas (Boswell *et al.*, 2012), and thus ~10 BCF low-salinity water.

Blake Ridge is a good analog for the GHSZ in the Mediterranean Sea as both contain poorly differentiated muddy sediments. Within a 30 m contour around the bathymetric high (about 2,600 km^2) in Blake Ridge, drilling has provided ground truth for wider estimates of NGH abundance, using seismic analysis, at about 37.7 trillion cubic feet (TCF) of gas with about 20 TCF gas trapped below the existing GHSZ (Dillon & Max, 2001). In seismic data, stronger amplitude reflection strength in the crest of Blake Ridge (and the apex of the base GHSZ) indicates that gas may have migrated from the flanks toward the apex of the structural ridge-crest trap (e.g., Vogt *et al.*, 1994). The BSR (Fig. 5) is imaged as a seismic event that often cuts across geological strata of fine-grained, poorly bed differentiated strata indicating its relatively younger age.

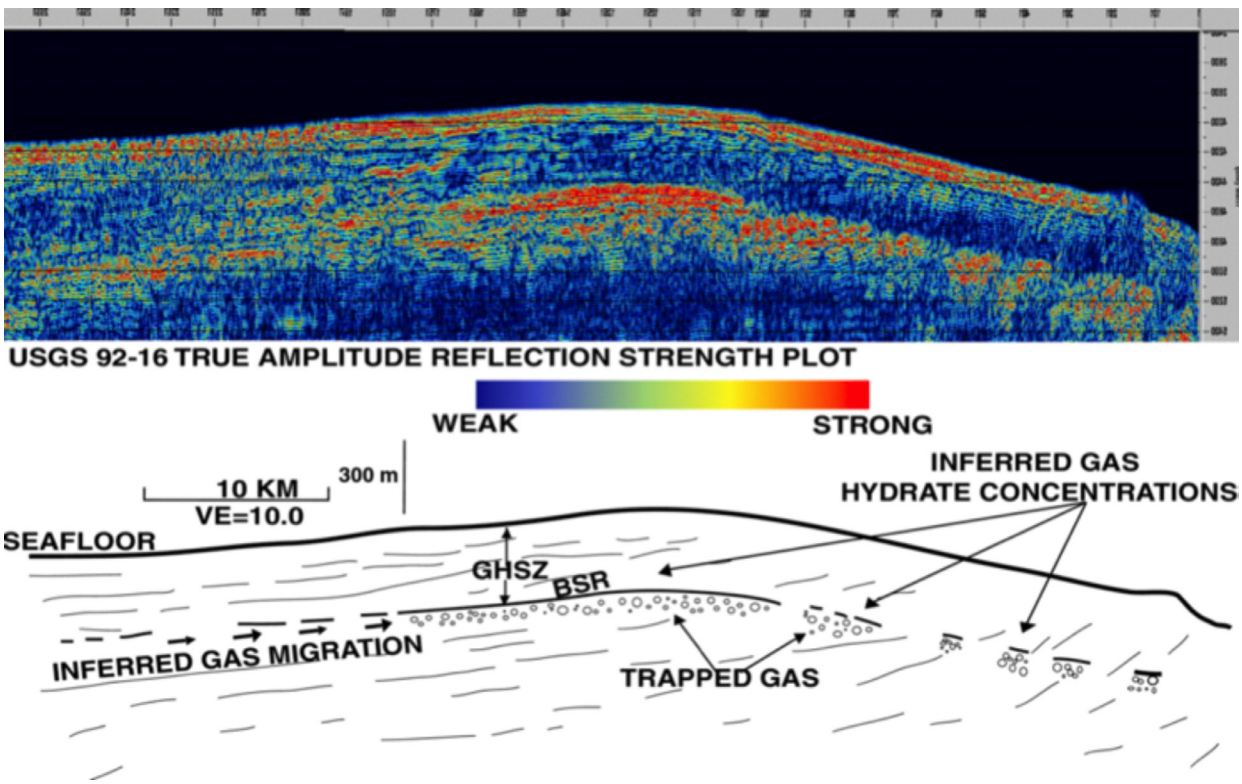

Fig. 5: Reflection seismic section across Blake Ridge of the US SE Coast. The BSR is picked at the junction between the low amplitude reflections overlying the higher amplitude reflection strength. From W.P. Dillon, U.S. Geological Survey.

Although the volumes for gas in place are large in those places where the estimates are based on both drilling and seismic valuation of NGH concentrations, the volume of associated NGH nearby not valued, because it is not regarded as being recoverable, results in conservative estimates of total volumes. Thus, even where NGH volume estimates are being made as part of NGH exploration, both the valued and additional NGH will produce gas and water once converted. Where large amounts of essentially unrecoverable NGH is held in concentrations of less than 10% in muddy reservoirs, such as on the Blake Ridge, conversion would produce low salinity water that has the potential to vent from the seafloor.

Natural Gas Hydrate and the Eastern Mediterranean Basin

NGH is responsive to slight environmental changes. During the Last Glacial Maximum (LGM) the modelled lower limit of a 4˚C decrease in seafloor water temperature resulted in the GHSZ migrating ~300 m up slope from its present day position and increasing in thickness

by ~25% (Praeg *et al.*, 2011). Since the LGM, seafloor warming has caused destabilization of NGH, and ponding of low-salinity water and natural gas, at the base GHSZ.

When sea level rises, as it has since the LGM, the pressure at the base of the GHSZ increases and tends to make NGH more stable, but increasing temperature overwhelms this and produces thinning of the GHSZ. Present day sea level is ~130 – 140 m above the LGM levels (Fairbanks, 1989; Clark & Tarasov, 2014; Lambeck *et al.*, 2014). This introduces pressure changes on the order of 10 – 15 atmospheres in subjacent marine sediments that may be important in relatively shallow water depths (e.g., Riboulot *et al.*, 2014) but would less affect sediments at depths 3 – 4 km below sea level in the Mediterranean Sea. The observation that mud volcanoes are more active during falls in sea level by Xing & Spiess (2015) is likely a function of increased permeability in the carrier systems and migration routes (Römer *et al.*, 2016) rather than significant pressure-driven changes in GHSZ thickness. Despite sea level rise present day changes in ocean temperature are driving GHSZ thinning (Mienert *et al.*, 2005).

Temperature changes through time follow glacial cycles; albeit with a lag time for NGH response that is mainly governed by the rate at which temperature changes propagate to the base GHSZ in deepwater. In near-surface sediments heat propagates downwards into the sediment pile at a rate of ~11 W/m/K (Della Vedova *et al.*, 2003), although large areas of salt produced during the Mediterranean Salinity Crisis complicate the heat flow framework owing to their high thermal conductivity. The gradual diffusion of heat through the sediment pile and the GHSZ acts as a low-pass filter to attenuate high frequency changes in seafloor temperature before they reach the base GHSZ, where they alter the NGH volume. Even so, due to the relatively large impact of a 1 – 4 ˚C change on hydrate at equilibrium at ~25 ˚C, seasonal (Berndt *et al.*, 2014), decadal (Dean *et al.*, 2015), and glacial cycles in NGH volume have been recognized.

Dynamics of Plume Propelled Vortex Tubes

Buoyant Fluid and Bubble Stream

Our new paradigm model for vent cored deep vortices that have not previously been related to the action of an NGH system is also based on a knowledge base of calculable effects. Multiphase buoyant plumes may ascend to different depths in the water column. The dominant controls are the momentum, buoyancy, and volume of emissions. In those instances in which gas and water migrate along a fault or other initiator (Fig. 4), the water plume can be expected to rise more rapidly. The gas and water will tend to separate and the gas will also dissolve when undersaturated seawater is available. Transport of gas through the GHSZ takes place commonly and is possibly in part the result of formation of NGH lining in fractures and vents. Because there appears to be so much venting of gas from seafloor at water depths well within the field of NGH stability, passage of gas is probably volumetrically larger than natural gas that becomes sequestered by the formation of NGH. Migration of gas in NGH will depend on the relative speed of the gas ascent and the rate of NGH formation; large volumes of free gas may then reach the seafloor (Max *et al.*, 2006).

The passage of these buoyant fluids in the water column is only beginning to be studied in detail so a clear link between vents and passage of material in the water column is not well understood. We document some of the relevant fluid mechanics parameters that can be used to quantitatively describe their ascent so that modeling of the relationship may be tested. The density of NGH-derived low-salinity water is lower than seawater because of its reduced salinity, dissolved natural gas, and microbubbles of natural gas that can be expected to form from ascending gas-saturated water. Columns of venting water/gas rise due to their buoyancy and momentum. Once vent water clears the seafloor, turbulence and drag decrease and the water column has the potential to remain coherent, with a sheath of essentially lamellar flow along its margins. Primarily, the buoyancy (B) flux that drives the rise of plumes in the water column can be described (Goodman *et al.*, 2004) as:

$$B = g \cdot (\delta\rho/\rho_{\alpha}) \cdot Q$$

Where g, standard gravity 9.8 m/s^2; δρ, density difference of plume fluid and seawater; ρ_a, density of seawater; Q, volumetric flow rate (m^3/sec).

In deep water at the seafloor, free gas volume would be relatively smaller than in shallower water for any particular volume of approximately equally saturated water. This means that at greater depths weaker buoyancy would result in increased potential for separation and fractionation of the dispersed and continuous phases where cross currents exist (Socolofsky & Adams, 2002). Provided that volume fluxes could be estimated or calculated accurately enough, the density of different fluids would be the most complex parameter to determine. Temperature (*T*), pressure (P), and the contraction coefficients for absolute salinity (S_A), dissolved CH_4 and CO_2 and gas volume per water volume (V_g) are all variables in the calculation of water densities involved in formation of plumes in the water column (adapted from Schmid *et al.*, 2004; Linke *et al.*, 2010):

$$\rho(T, P, S_A, V_{CO_2}, V_{CH_4}) = \rho(T) \cdot (1+\beta^t (S_A, T, P) + \beta_{CO_2} \cdot V_{CO_2} + \beta_{CH_4} \cdot V_{CH_4}) \cdot (1-V_g (P))$$

Where *V,* volume, V_g, volume gas per volume water, β^t, contraction coefficient of seawater, S_A, the absolute salinity can be defined McDougall *et al.* (2010). CO_2 increases the density of water as it has a positive contrac-

tion coefficient (βCO_2 = 0.24) whereas dissolved CH_4 has a negative contraction coefficient (βCH_4 = -1.25); greater volumes of dissolved methane in a plume would result in greater plume buoyancy and even small density contrasts can drive ascension.

Drag Zone between Vortex and Seawater

Where specific circumstances exist ascending-buoyant fluid forms vortices. The outer contour of the vortex stream can be represented by lines of rotational flow at the boundary between the outer tightly wound spiral layer of the vortex and the unrolled-up seawater (Saffman, 1992). This outermost layer of the vortex forms a tube-shape drag zone where seawater is slowly entrained into the ascending stream. The result of these forces is that the water movement and vertical drag produce localized rotational momentum.

Drag at the edge of the plume is responsible for mixing inward from the margin of the plume via the entrainment coefficient α_e, a constant proportional to the velocity at a particular elevation (Carazzo *et al.*, 2008):

$$\alpha_e = \frac{C}{2} + \left(1 - \frac{1}{A}\right) Ri + \frac{R}{2}\frac{\partial \ln B}{\partial z}$$

$$Ri = RU^2$$

Where Ri is the Richardson number and C = shear stress, parameters A and B depend on flow properties, and specifically describe the shapes of velocity, buoyancy, and turbulent shear stress profiles while in the upper plume *R* = radius and *U* = velocity (Carazzo *et al.*, 2008).

$$C = -6(1 + \lambda^2) \int_0^\infty r^* \exp(-r^{*2})\, j(r^*) \delta r^*$$

Where: λ, ratio buoyancy: velocity profiles; j, turbulent shear stress; $r^* = r / b_m$; b_m, radius scale.

As the plume ascends, fluid with a reduced saturation of the molecular gas species would be slowly incorporated into the vortex tube. Without mixing with surrounding water, NGH-shelled bubbles have extended lifetimes due to their lower dissolution rates (Rehder *et al.*, 2002). Because the drag zone effectively separates dissolved gas-rich core water from the surrounding ambient seawater, mixing of reduced saturation seawater into the vortex core waters is unlikely to result in dissolution of NGH (Rehder *et al.*, 2004). NGH within the core vortex waters would be largely bubble shells and fragmental shell masses, especially where the dissolved natural gas is close to saturation.

Vortex Tube Propellant

Plume rotation can be initiated by the interaction of Coriolis forces where they are large enough to overcome inertia and impart motion. Coriolis force associated with longer lasting emissions has the potential to produce higher speed and broader rotational elements.

The ratio of inertial to Coriolis forces is described by the Rossby number:

$$R_o = \frac{inertial\ forces}{Coriolis\ forces}$$

The Rossby number can be expressed as:

$$R_o = \frac{U}{Lf}$$

Where: *U*, flow velocity; *L*, length scale; *f*, Coriolis parameter:

$$f = 2\,\Omega\, sin\varphi$$

Where: Ω, angular velocity of planetary rotation; φ, latitude.

When R_o is ~1 both inertial and Coriolis forces are important. When R_o is greater than 1 inertial force dominates and when it is less than 1 Coriolis dominates. Expressed another way, rotation is more likely where vent orifices are larger and flow velocity smaller. A plume similar to that observed by Rubino *et al.* (2012) with an average velocity value U ~10 cm/s, diameter of emissions *L* ~1.5 km, and *f* ~2π/24/hr. has an R_o value of ~0.9. This means that Coriolis force is likely to be dominant and also predicts that ascending fluids would rotate.

Based on laboratory experiments of plume height, Bush & Woods (1999) show that water depth is an important variable in plume rotation. When water depth is greater than ten times the height of the rotating plume $Wd > 10H$, the ascent phase of the plume would tend to include rotation. However, if $Wd < 10H$, the plume ascent would not feature rotation. Although, vortices are not predicted to form in shallow water, where the plumes are initially constrained by physical barriers such as a crater or fault walls in the seafloor; vectoring of water direction can result in a wandering, spiral, or transient morphology (Pfleger *et al.*, 1999). In this case, rotation is related to asymmetrical or steering injection, characterized by a decrease in rotational momentum and increased mixing away from the vent orifice.

In deep water the timescales for plume ascent and the inertial period are similar (hours). If the ascent time of a plume is similar to the rotation period then fluid in the plume would rotate and begin to form a vortex tube. At an average ascent velocity of 10 cm/s, an entrained particle would ascend at ~360 m/hour. This means that in water depths deeper than ~1000 m the timescale of ascent is similar to that of the rotation period: $t_\alpha = t_\Omega$.

Formation of Vortex Dipoles

The creation of line plumes (Bush & Woods, 1999) can be theoretically modeled in both Eulerian and Langrangian terms. In the case of an Eulerian system, a current moves over a stationary point source with intermittent ebullition. In contrast, in a Langrangian system, a line-source plume is emitted along a line source into a unidirectional fluid that is essentially stationary at the time of the emissions. In both cases and considering that the release of emissions is not continuous, the number of vortices to form would be (Bush & Woods, 1999):

$$n = C_1 \frac{{L_f}^{1/2}}{t_s^{1/2} B^{1/3}}$$

Where t_s, source time; C_1 is a constant equal to 0.65 ± 0.1.

Anticyclone – cyclone – anticyclone chains can be created by either continuous emissions that create anticyclonic vortices that spin up concomitant cyclonic vortices or when width/Rossby radius of rotational deformation is greater than 1 ($W / R > 1$), (Griffiths *et al.*, 1982).

Vortex Tube Spin Down

Plumes eventually spin-down over a timescale controlled by physical parameters (Hedstrom & Armi, 1988; Bush & Woods, 1999), where h, half-height of a plume, v, viscosity:

$$\tau_s \sim h/(\Omega v)^{1/2}$$

Spin-down describes the rate at which momentum will be lost such that an oceanic vortex with a radius of ~5 km could travel ~600 km through the Mediterranean over the course of a year at a current transport rate of 1.9 cm/s (Bush & Woods, 1999). This timescale is similar to Mediterranean eddies (Rubino *et al.*, 2012).

Axialized Plumes in Vortex Tubes

Acoustic images of ascending gas and fluids in the water column show that they tend to form tight axial columns instead of spreading out as they rise. We suggest that where venting is sufficiently persistent and focused, the buoyant stream rotary motion can affect concentration of more buoyant elements within the plume. Fluid motion aligned with the rotation axis and driven by buoyancy of the fluid, gas, fragmental NGH mass, and Coriolis acceleration create centripetal forces that would cause buoyant matter to move toward the core of the stream. The core region would then be a multiphase mixture of: 1) low temperature, low-salinity, water and dissolved gas, 2) gas bubbles, 3) bubble shells, and 4) fragmental NGH, all of which have a lower density than the surrounding water (Fig. 6). The density differences would drive a centripetal force that causes the plume to be more coherent and increase the buoyant force by concentrating and isolating buoyant phases towards the core. Rotation of the plume would tend to create vortex stability and prevent breakup.

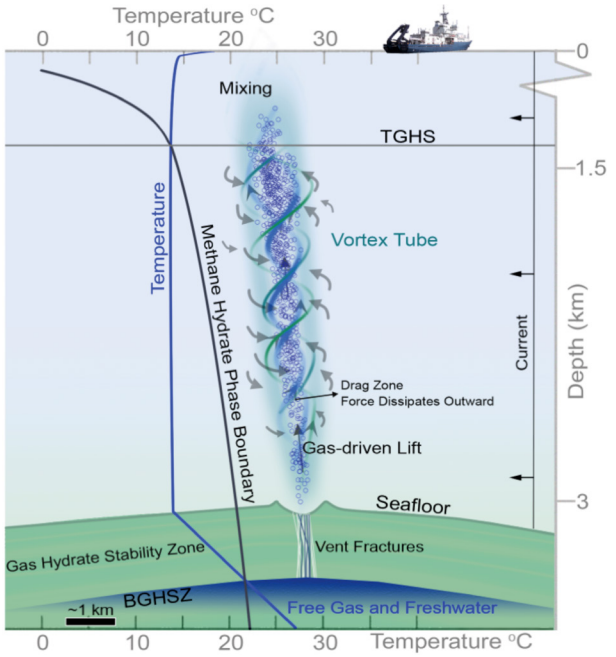

Fig. 6: Diagram of buoyant plume initiating a vortex tube due to Coriolis acceleration and centripetal forces that drive the buoyant NGH shelled bubbles, and fragmental mass of NGH shell flakes, toward the center of the tube. Before reaching the top GHS widespread dissociation of NGH occurs in conjunction with dissolution before mixing of the plume water with surface waters.

The drag zone that separates the vortex tube from the surrounding seawater exerts a bounding force on the tube and assists in maintaining its shape. Undirected hydrostatic pressures decrease during bubble ascent resulting in gas exsolution and bubble expansion and fragmentation, which in turn results in increased buoyancy, possible expansion of the bubble plume, and changes in the interfacial tension of hydrate-shelled bubbles. Vortex tube generation could explain the consistent relatively slender morphologies associated with plumes seen in multibeam data (Solomon *et al.*, 2009; Colbo *et al.*, 2014; Skarke *et al.*, 2014; Smith *et al.*, 2014; Tudino *et al.*, 2014; Weber *et al.*, 2014; Garcia-Pineda *et al.*, 2015; Wilson *et al.*, 2015) and recent observations indicate that vertical rise of buoyant plumes may be augmented by spiral flow geometries (von Deimling *et al.*, 2015). Because the reflection and scattering from a bubble plume is a bulk effect, rotation has not been observed in seismic reflection data. In many cases the plumes can be seen to change direction for a short duration of their ascent only to return to their

original trajectory after a short time, which is attributed to bending of the vortex tube by currents in a stratified ocean.

Discussion and Conceptual Model

We propose that a direct relationship may exist between the formation of low salinity water and gas at relatively shallow sediment depths, its potential for mass venting, and the consequent formation of water-cored large-scale deepwater vortices. Due to its low latitude, relatively small size, and isolation from the Atlantic cold deep water, the Mediterranean Sea is a natural laboratory for observing the effects of temperature variation from glacial to interglacial conditions on the GHSZ. Like the Arctic Ocean, due to its particular geography and location, the effects of ocean temperature changes since the last glacial period (e.g., Bindoff *et al.*, 2007) have a greater impact than elsewhere (Biastoch *et al.*, 2011) and allow further analysis of the effects of climate forcing of NGH (e.g., Archer, 2007; Kretschmer *et al.*, 2015). Temperature changes typically induce heterogeneous changes in the Mediterranean Sea, but in recent years ecological responses have been at the basin-scale (Rivetti *et al.*, 2014) indicating an increase in the rate of change and making the Mediterranean Sea a possible model for the GHSZ in open ocean conditions under the high-end IPCC representative concentration pathway scenarios (Pachauri & Reisinger, 2007; Pachauri *et al.*, 2014).

During the LGM, the GHSZ was over ~500 m thick in the vicinity of the vortices reported by Rubino *et al.* (2012) whereas the present GHSZ is only ~200 to 300 m thick (Praeg *et al.*, 2011). As it can be expected that most of the NGH will be in the lower third of the GHSZ, large volumes of NGH have been, and probably continue to be, converted to constituent gas and water. Dissociation of NGH in marine sediments introduces active dynamic forces and potential for a refrigeration effect into deep marine environments that are traditionally characterized as passive, potentially also opening some sedimentary deformation in the geological record to reinterpretation (e.g., Max & Johnson, 2012; Robinson *et al.*, 2015).

Praeg *et al.* (2011) suggest that the faulting and sediment mass flows in the 700 – 1000 m depth interval of the was a result of massive NGH conversion owing to Mediterranean Sea warming that they regard as largely completed by about 10,000 BP. It is not possible to know what percentage or amount of NGH was converted during the early or subsequent thinning of the GHSZ, but we can postulate that significant amounts of low-salinity water and free gas were produced as a result of NGH dissociation (Max *et al.*, 2006) and that considerable amounts of low salinity water may still be held within the sediment. Although more quantitative estimates for NGH products, such as those conducted in Svalbard and the Cascadia margin (Berndt *et al.*, 2014; Hautala *et al.*, 2014), remain to be carried out for the Mediterranean (Max & Johnson, 2016), conversion of a large amount of NGH into low-salinity water and gas is highly likely.

Accumulation of low-salinity water and gas at the base GHSZ creates a positively buoyant pond of pore water that will exert upward pressure against the retention capacity of the suprajacent host sediments, whose permeability is reduced due to NGH replacement of pore water. Within a GHSZ in a sediment ridge, gas may become concentrated in pseudo-anticlinal forms at the base GHSZ (Vogt *et al.*, 1994). The degree of NGH displacement of pore water decreases with depth (Max & Dillon, 1998). Because gas overpressures can be significant if NGH conversion exceeds pressure re-equilibration by groundwater displacement, a strong dynamic force in the subsurface marine sediments could be generated where only quiescent, gently dewatering sediments might otherwise be expected. In order to generate a coherently flowing multiphase mass, a large volume of gas-saturated low salinity water would have to be released into deep water over a relatively short period of time.

Fluids and gases that are produced at an unstable base of a GHSZ would tend be at the local ambient temperature if rising temperature were the cause of conversion. Water rising through the GHSZ could be cooled by direct heat exchange as it rose toward the seafloor. The longer the multiphase fluid takes to rise to the seafloor, the closer to the temperature of the seafloor water would be attained. In contrast, if pressure drop were the cause of conversion, potential for substantial cooling would exist. Because free gas in the fluidized mass would expand as it rises, some cooling could also be expected owing to the action of Charles' Law governing volume / temperature / pressure. Depending on the cause of conversion, the rate of ascent, and the ratio of gas to low-salinity water in the seafloor vent, water released from the seafloor could be at a lower temperature than seafloor water.\

As the gas saturated waters rise free gas bubbles form and the formation and morphology of hydrate shells is controlled by midwater thermo-hydrodynamics (Warzinski *et al.*, 2014; Levine *et al.*, 2015). As bubbles ascend a balance exists between the gains made by reduced diffusion and dissolution by the presence of NGH shells on bubbles versus their relatively longer and more complex ascent during the transport process of gas through the water column (Li & Huang, 2016). NGH bubble shells may dissolve prior to reaching the top GHS if they encounter sufficiently undersaturated seawater within the vortex (Chen *et al.*, 2013; Warzinski *et al.*, 2014; Levine *et al.*, 2015).

During buoyant rise, free gas would continue to exsolve from the supersaturated low-salinity water. A theoretical maximum based on calculation of the percent methane volume / water volume yields a ratio of 1:9.6, meaning that based on approximate value for a 100 m^3

volume of Mediterranean seawater ascending from 3000 m to surface waters, exsolution of methane would provide a gas volume of approximately 960 m^3 (Yamamoto *et al.*, 1976; Wang *et al.*, 2010). Because vaporization is about 18 kJ/mol (Max & Johnson, 2011), the effects would be felt within the water mass as a whole, and the low-salinity water would be cooled further prior to separation of the more buoyant gas from the water. A 100 m^3 volume of deep water contains ~700 kg (1.7 m^3) methane that requires ~800 kJ energy for the molar heat of vaporization, which is equivalent to a drop in temperature of ~2 ˚C for exsolution of all the methane from the 100 m^3 volume. Formation of a gas phase from the supersaturated low-salinity water would persist during the ascent of the plume. As pressure decreased with decreasing water depth, the low-salinity water in the plume would continue to effuse gas and to cool, even if gas bubbles were too small to be visible or to dramatically affect seismic response. At the same time, Charles' Law effect chilling would also persist. Because of the difference in buoyancy, and unless the plume is in a 'fluidized' state in which water and gas are so intermixed by turbulence that separation of water and gas is inhibited, free gas would tend to separate from the cooling low-salinity water.

Although the gas effect in a water plume could also drive plume buoyancy and cooling, if the water from a vent has a lower salinity than would be anticipated from normal pore water deposited in deep marine conditions, then we suggest that the water would likely have been produced, at least in part, from NGH dissociation. This episodic, overpressure-generated NGH mechanism for generating buoyant plumes at any water depth below which NGH is stable in the Mediterranean Basin would provide a local source of cooler low-salinity water for vortex cores. The same effect may be found in other seas and oceans. Low-salinity water derived from NGH may also be a mechanism for enhanced fluid flow that sustains benthic communities (Mayer *et al.*, 1988; Ryan, 2009; Carey *et al.*, 2014), and bubble-mediated transport within plumes that provides a mechanism for deep sea communities to reach and interact with pelagic communities (Schmale *et al.*, 2015). Monitoring and sampling of deep-sea fluid and gas emission sites should resolve our model for a dynamic source for deep-water mixing.

Rotary circulation within a gas plume would be best characterized by chemical, temperature, optical, and acoustic observations recorded through shipboard, ROV, and AUV platforms in the water column adjacent to, and within, plumes. It is suggested that carefully located deep ADCP may be able to resolve a rotation within a plume and could be used to test our suggestion that maintenance of the tight axial shape of the plumes is at least partially due to the formation of a vortex tube. Multibeam sonar data may also be useful for determining some of the plume internal structure and rotation (e.g., von Deimling *et al.*, 2015; Wilson *et al.*, 2015). Instrumentation specifically set up for volumetric water mass assessment, or a number of AUVs having very sensitive internal navigation would be needed to identify plume morphology and rotation.

Conclusions

We propose that the anomalously cold water cores of deep ocean vortices of Rubino *et al.* (2012) are related to large releases of low-salinity, low-temperature, water produced as a result of the dissociation of NGH in near-surface sediments. Deriving low-salinity water from relatively shallow depths below the deep seafloor is a simpler explanation than by somehow bringing low density near-surface water to abyssal depths from great distances, a process that has not been observed during a century of oceanography in the region.

Deepwater NGH formation provides a long-term mechanism for sequestering large volumes of low-salinity water in crystalline NGH over an extensive period of time. Dissociation at the base of the GHSZ as the seafloor warms (e.g., during the onset of interglacial conditions) would produce low-salinity water along with hydrate-forming gas that would pond at the base GHSZ. Even without very buoyant gas as a driver, the water masses low-salinity increases its buoyancy, especially if saturated with methane and free gas. When the low-salinity water mass is released into the sea, it would tend to rise as a mass, creating turbulence at its contacts with the more saline seawater. During ascent the ponded water moving up through the GHSZ and into seawater cools by direct heat exchange. The vent water supersaturated with gas rising with free gas cools in midwater by expansion and vaporization. The cooling processes have the potential to produce vent water plugs that are cooler than the ambient seawater. The buoyancy of the chilled plume drives its ascent, and the consequent stabilization of their form by rotation is a result of forces generated by buoyant rise and Coriolis acceleration. The creation of vortex tubes around buoyant plumes in the water column could explain the characteristic morphologies of some acoustic flares seen in multibeam images. Colder-water cores of deep-ocean vortices (e.g., Rubino *et al.*, 2012) could be formed by emissions of low-salinity and temperature water vented from the seafloor.

NGH is formed and converted by a highly reversible chemical reaction and is very responsive to changes in the thermal and pressure state of its surroundings. This conversion process in the abandoned lower GHSZ may still be active if warming is still active. If the Mediterranean seafloor warms further, for instance owing to warming of deep Mediterranean waters, the base of the GHSZ could be expected to further shallow, converting more NGH to low-salinity water and gas. Periodic release of the low-salinity water from sediments in the Eastern Mediterra-

nean Basin immediately to the SE of Sicily could be the source of the low-salinity water cores of recently recognized deep-sea oceanographic current vortices.

References

Adrián-Martínez, S., Ageron, M., Aharonian, F., Aiello, S., Albert, A. *et al.*, 2016. The prototype detection unit of the KM3NeT detector. *The European Physical Journal, C* 76, 1-12.

Adrián-Martínez, S., Ageron, M., Aharonian, F., Aiello, S., Albert, A. *et al.*, 2014. Deep sea tests of a prototype of the KM3NeT digital optical module. *The European Physical Journal, C* 74, 3056.

Aloisi, G., Pierre, C., Rouchy, J.-M., Foucher, J.-P., Woodside, J., 2000. Methane-related authigenic carbonates of eastern Mediterranean Sea mud volcanoes and their possible relation to gas hydrate destabilisation. *Earth and Planetary Science Letters,* 184, 321-338.

Archer, D., 2007. Methane hydrate stability and anthropogenic climate change. *Biogeosciences Discussions,* 4, 993-1057.

Aynutdinov, V., Kindin, V., Kiselev, S., Petrukhin, A., Potapov, G. *et al.*, 1995. Present Status of the NESTOR Project, International Cosmic Ray Conference, p. 1076.

BBC, 2009. HD: Super Slo-mo Surfer! - South Pacific - BBC Two https://www.youtube.com/watch?v=7BOhDaJH0m4 (25 January 2016).

Berndt, C., Feseker, T., Treude, T., Krastel, S., Liebetrau, V. *et al.*, 2014. Temporal constraints on hydrate-controlled methane seepage off Svalbard. *Science,* 343, 284-287.

Biastoch, A., Treude, T., Rüpke, L.H., Riebesell, U., Roth, C. *et al.*, 2011. Rising Arctic Ocean temperatures cause gas hydrate destabilization and ocean acidification. *Geophysical Research Letters,* 38.

Bindoff, N.L., Willebrand, J., Artale, V., Cazenave, A., Gregory, J.M. *et al.*, 2007. Observations: oceanic climate change and sea level. p. 385–432. In: *Climate Change 2007: The Physical Science Basis. Contribution of Working Group I to the Fourth Assessment Report of the Intergovernmental Panel on Climate Change. Intergovernmental Panel on Climate Change*. Solomon, S., Qin, D., Manning, M., Chen, Z., Marquis, M., Averyt, K.B., Tignor, M., Miller, H.L. (Eds). Cambridge University Press, Cambridge, United Kingdom and New York, NY, USA.

Boswell, R., Frye, M., Shelander, D., Shedd, W., McConnell, D.R. *et al.*, 2012. Architecture of gas-hydrate-bearing sands from Walker Ridge 313, Green canyon 955, and Alaminos canyon 21: northern deepwater Gulf of Mexico. *Marine and Petroleum Geology,* 34, 134-149.

Bush, J.W., Woods, A.W., 1999. Vortex generation by line plumes in a rotating stratified fluid. *Journal of Fluid Mechanics,* 388, 289-313.

Carazzo, G., Kaminski, E., Tait, S., 2008. On the rise of turbulent plumes: Quantitative effects of variable entrainment for submarine hydrothermal vents, terrestrial and extra terrestrial explosive volcanism. *Journal of Geophysical Research: Solid Earth (1978–2012),* 113, 10.1029/2007JB005458.

Carey, S., Ballard, R., Bell, K.L., Bell, R.J., Connally, P. *et al.*, 2014. Cold seeps associated with a submarine debris avalanche deposit at Kick'em Jenny volcano, Grenada (Lesser Antilles). *Deep Sea Research Part I: Oceanographic Research Papers,* 93, 156-160.

Chen, L., Sloan, E.D., Koh, C.A., Sum, A.K., 2013. Methane hydrate formation and dissociation on suspended gas bubbles in water. *Journal of Chemical & Engineering Data,* 59, 1045-1051.

Chierici, F., Favali, P., Beranzoli, L., De Santis, A., Embriaco, D. *et al.*, 2012. NEMO-SN1 (Western Ionian Sea, off Eastern Sicily): a cabled abyssal observatory with tsunami early warning capability. p. 130-137. In: *Proceedings 22nd International Off-shore and Polar Engineering Conference*, International Society of Off-shore and Polar Engineers (ISOPE).

Clark, P.U., Tarasov, L., 2014. Closing the sea level budget at the Last Glacial Maximum. *Proceedings of the National Academy of Sciences,* 111, 15861-15862.

Colbo, K., Ross, T., Brown, C., Weber, T., 2014. A review of oceanographic applications of water column data from multibeam echosounders. *Estuarine, Coastal and Shelf Science,* 145, 41-56.

Dählmann, A., 2005. Gas hydrates in the Eastern Mediterranean: occurrence and biogeochemical environment compiled from detailed sampling of the Anaximander Mountains. *Geophysical Research Abstracts,* 7, 05176.

De Lange, G., Brumsack, H.-J., 1998. The occurrence of gas hydrates in Eastern Mediterranean mud dome structures as indicated by pore-water composition. *Geological Society, London, Special Publications,* 137, 167-175.

Dean, W.E., Kennett, J.P., Behl, R.J., Nicholson, C., Sorlien, C.C., 2015. Abrupt termination of Marine Isotope Stage 16 (Termination VII) at 631.5 ka in Santa Barbara Basin, California. *Paleoceanography,* 30, 1373-1390.

Della Vedova, B., Pellis, G., Camerlenghi, A., Foucher, J.-P., Harmegnies, F., 2003. Thermal history of deep-sea sediments as a record of recent changes in the deep circulation of the eastern Mediterranean. *Journal of Geophysical Research: Oceans (1978–2012,)* 108, 10.1029/2002JC001402.

Dillon, W.P., Max, M.D., 2001. The US Atlantic continental margin; the best-known gas hydrate locality. p. 157-170 In: *Natural Gas Hydrates: Occurrence, Distribution, and Detection*. Paull, C.K., Dillon, W.P. (Eds). Springer, Washington, D. C.

Fairbanks, R.G., 1989. A 17, 000-year glacio-eustatic sea level record: influence of glacial melting rates on the Younger Dryas event and deep-ocean circulation. *Nature,* 342, 637-642.

Feder, T., 2002. Deep-sea Km3 neutrino detector gets thumbs up. *Physics Today,* 55, 20-21.

Garcia-Pineda, O., MacDonald, I., Silva, M., Shedd, W., Asl, S.D. *et al.*, 2015. Transience and persistence of natural hydrocarbon seepage in Mississippi Canyon, Gulf of Mexico. *Deep Sea Research Part II: Topical Studies in Oceanography,* 129, 119-129.

Goodman, J.C., Collins, G.C., Marshall, J., Pierrehumbert, R.T., 2004. Hydrothermal plume dynamics on Europa: Implications for chaos formation. *Journal of Geophysical Research,* 109, 10.1029/2003JE002073.

Griffiths, R., Killworth, P.D., Stern, M.E., 1982. A geostrophic instability of ocean currents. *Journal of Fluid Mechanics,* 117, 343-377.

Hautala, S.L., Solomon, E.A., Johnson, H.P., Harris, R.N., Miller, U.K., 2014. Dissociation of Cascadia margin gas hydrates in response to contemporary ocean warming. *Geophysical Research Letters,* 41, 8486-8494.

Hedstrom, K., Armi, L., 1988. An experimental study of homogeneous lenses in a stratified rotating fluid. *Journal of Fluid Mechanics,* 191, 535-556.

Hesse, R., 2003. Pore water anomalies of submarine gas-hydrate zones as tool to assess hydrate abundance and distribution in the subsurface: What have we learned in the past decade? *Earth-Science Reviews,* 61, 149-179.

Holbrook, W.S., 2001. Seismic studies of the Blake Ridge: Implications for hydrate distribution, methane expulsion, and free gas dynamics. *Natural gas hydrates*, 235-256.

JOGMEC, 2013. Gas production from methane hydrate layers confirmed. http://www.jogmec.go.jp/english/news/release/release0110.html

Katz, U.F., 2006a. KM3NeT: towards a km 3 Mediterranean neutrino telescope. *Nuclear Instruments and Methods in Physics Research Section A: Accelerators, Spectrometers, Detectors and Associated Equipment,* 567, 457-461.

Katz, U.F., 2006b. Neutrino telescopy in the Mediterranean sea. *Progress in Particle and Nuclear Physics,* 57, 273-282.

Katz, U.F., KM3NeT-consortium, 2009. Status of the KM3NeT project. *Nuclear Instruments and Methods in Physics Research Section A: Accelerators, Spectrometers, Detectors and Associated Equipment,* 602, 40-46.

Kretschmer, K., Biastoch, A., Rüpke, L., Burwicz, E., 2015. Modeling the fate of methane hydrates under global warming. *Global Biogeochemical Cycles,* 29, 610-625.

Lambeck, K., Rouby, H., Purcell, A., Sun, Y., Sambridge, M., 2014. Sea level and global ice volumes from the Last Glacial Maximum to the Holocene. In: *Proceedings of the National Academy of Sciences* 111, 15296-15303.

Levine, J.S., Haljasmaa, I., Lynn, R., Shaffer, F., Warzinski, R.P., 2015. Detection of Hydrates on Gas Bubbles during a Subsea Oil/Gas Leak, EPAct Technical Report Series. U.S. Department of Energy, National Energy Technology Laboratory: Pittsburgh, PA,, p. 44.

Li, C., Huang, T., 2016. Simulation of gas bubbles with gas hydrates rising in deep water. *Ocean Engineering,* 112, 16-24.

Linke, P., Sommer, S., Rovelli, L., McGinnis, D.F., 2010. Physical limitations of dissolved methane fluxes: The role of bottom-boundary layer processes. *Marine Geology,* 272, 209-222.

Loncke, L., Mascle, J., Parties, F.S., 2004. Mud volcanoes, gas chimneys, pockmarks and mounds in the Nile deep-sea fan (Eastern Mediterranean): geophysical evidences. *Marine and Petroleum Geology,* 21, 669-689.

Lykousis, V., Alexandri, S., Woodside, J., De Lange, G., Dählmann, A. *et al.*, 2009. Mud volcanoes and gas hydrates in the Anaximander mountains (Eastern Mediterranean Sea). *Marine and Petroleum Geology* 26, 854-872.

Marinakis, D., Varotsis, N., Perissoratis, C., 2015. Gas hydrate dissociation affecting the permeability and consolidation behaviour of deep sea host sediment. *Journal of Natural Gas Science and Engineering,* 23, 55-62.

Max, M., Dillon, W.P., 1998. Oceanic methane hydrate: the character of the Blake Ridge hydrate stability zone, and the potential for methane extraction. *Journal of Petroleum Geology,* 21, 343-357.

Max, M., Johnson, A., 2011. Methane hydrate/clathrate conversion. *Advances in Clean Hydrocarbon Fuel Processing: Science And Technology. Woodhead Publishing Series in Energy*, 413-434.

Max, M.D., Johnson, A.H., 2012. NGH: A dynamic factor in deep water sediments & the geological record, AGU Fall Meeting, San Francisco.

Max, M.D., Johnson, A.H., 2016. Exploration and Production of Oceanic Natural Gas Hydrate: Critical Factors for Commercialization. Springer International Publishing.

Max, M.D., Johnson, A.H., Dillon, W.P., 2006. Economic geology of natural gas hydrate. Springer.

Mayer, L., Shor, A., Clarke, J.H., Piper, D., 1988. Dense biological communities at 3850 m on the Laurentian Fan and their relationship to the deposits of the 1929 Grand Banks earthquake. *Deep Sea Research Part A. Oceanographic Research Papers,* 35, 1235-1246.

McDougall, T.J., Feistel, R., Wright, D.G., Pawlowicz, R., Millero, F.J. *et al.*, 2010. The international thermodynamic equation of seawater-2010: Calculation and use of thermodynamic properties, Manuals and Guides. UNESCO, Intergovernmental Oceanographic Comission, p. 196.

Mienert, J., Vanneste, M., Bünz, S., Andreassen, K., Haflidason, H. *et al.*, 2005. Ocean warming and gas hydrate stability on the mid-Norwegian margin at the Storegga Slide. *Marine and Petroleum Geology,* 22, 233-244.

Pachauri, R., Reisinger, A., 2007. IPCC fourth assessment report. *IPCC, Geneva*, 2007.

Pachauri, R.K., Allen, M.R., Barros, V.R., Broome, J., Cramer, W. *et al.*, 2014. Synthesis Report. Contribution of Working Groups I, II and III to the Fifth Assessment Report of the Intergovernmental Panel on Climate Change. p. 151. In: *Climate Change 2014*. Meyer, R.P.a.L. (Ed),. Intergovernmental Panel on Climate Change, Geneva, Switzerland.

Paull, C., Borowski, W., Rodriguez, N., 1998. Marine gas hydrate inventory: preliminary results of ODP Leg 164 and implications for gas venting and slumping associated with the Blake Ridge gas hydrate field. *Geological Society, London, Special Publications,* 137, 153-160.

Paull, C.K., Matsumoto, R., Wallace, P.J., 1996. Leg 164 Overview. p. 5-12. In: *Proceedings of the Ocean Drilling Program: Scientific Results. ODP*.

Paull, C.K., Ussler, W., 2001. History and significance of gas sampling during DSDP and ODP drilling associated with gas hydrates. p. 53-65. In: *Natural Gas Hydrates: Occurrence, Distribution, and Detection. American Geophysical Union*. Paull, C.K., Dillon, W.P. (Eds). Washington, D. C.,

Perissoratis, C., Ioakim, C., Alexandri, S., Woodside, J., Nomikou, P. *et al.*, 2011. Thessaloniki mud volcano, the shallowest gas hydrate-bearing mud volcano in the Anaximander Mountains, Eastern Mediterranean. *Journal of Geological Research,* Article ID 247983, doi:10.1155/2011/247983.

Pfleger, D., Gomes, S., Gilbert, N., Wagner, H.-G., 1999. Hydrodynamic simulations of laboratory scale bubble columns fundamental studies of the Eulerian–Eulerian

modelling approach. *Chemical Engineering Science,* 54, 5091-5099.

Piattelli, P., NEMO-collaboration, 2005. The neutrino mediterranean observatory project. *Nuclear Physics B-Proceedings Supplements,* 143, 359-362.

Pierre, C., Rouchy, J.-M., 2004. Isotopic compositions of diagenetic dolomites in the Tortonian marls of the western Mediterranean margins: evidence of past gas hydrate formation and dissociation. *Chemical Geology,* 205, 469-484.

Post, V.E., Groen, J., Kooi, H., Person, M., Ge, S. *et al.*, 2013. Offshore fresh groundwater reserves as a global phenomenon. *Nature,* 504, 71-78.

Praeg, D., Geletti, R., Wardell, N., Unnithan, V., Mascle, J. *et al.*, 2011. The Mediterranean Sea: A natural laboratory to study gas hydrate dynamics? p. 8. In: *Proceedings of the 7th International Conference on Gas Hydrates (ICGH 2011)*, Edinburgh, Scotland, United Kingdom,.

Rehder, G., Brewer, P.W., Peltzer, E.T., Friederich, G., 2002. Enhanced lifetime of methane bubble streams within the deep ocean. *Geophysical Research Letter,s* 29, 21-24.

Rehder, G., Kirby, S.H., Durham, W.B., Stern, L.A., Peltzer, E.T. *et al.*, 2004. Dissolution rates of pure methane hydrate and carbon-dioxide hydrate in undersaturated seawater at 1000-m depth. *Geochimica et Cosmochimica Acta,* 68, 285-292.

Rhein, M., Rintoul, S., Aoki, S., Campos, E., Chambers, D. *et al.*, 2013. Chapter 3: Observations: Ocean. p. 255-316. In: *Climate Change 2013: The Physical Science Basis. Contribution of Working Group I to the Fifth Assessment Report of the Intergovernmental Panel on Climate Change*. Stocker, T.F., Qin, D., Plattner, G.-K., Tignor, M., Allen, S.K., Boschung, J., Nauels, A., Xia, Y., Bex, V., Midgley, P.M. (Eds), Cambridge University Press, Cambridge, United Kingdom and New York, NY, USA.

Riboulot, V., Thomas, Y., Berné, S., Jouet, G., Cattaneo, A., 2014. Control of Quaternary sea-level changes on gas seeps. *Geophysical Research Letters,* 41, 4970-4977.

Rivetti, I., Fraschetti, S., Lionello, P., Zambianchi, E., Boero, F., 2014. Global Warming and Mass Mortalities of Benthic Invertebrates in the Mediterranean Sea. *PloS one,* 9, e115655.

Roberts, H.H., Hardage, B.A., Shedd, W.W., Hunt Jr, J., 2006. Seafloor reflectivity—an important seismic property for interpreting fluid/gas expulsion geology and the presence of gas hydrate. *The Leading Edge,* 25, 620-628.

Robinson, K., Kackstaetter, U., Echohawk, B., 2015. The Origin of a Layer of Subcircular Mudflakes in the Ross Sandstone Formation of County Clare, Ireland, AGU Fall Meeting. AGU, San Francisco.

Römer, M., Riedel, M., Scherwath, M., Heesemann, M., Spence, G.D., 2016. Tidally controlled gas bubble emissions: A comprehensive study using long-term monitoring data from the NEPTUNE cabled observatory offshore Vancouver Island. *Geochemistry, Geophysics, Geosystems,* 17, 3797-3814.

Rubino, A., Falcini, F., Zanchettin, D., Bouche, V., Salusti, E. *et al.*, 2012. Abyssal undular vortices in the Eastern Mediterranean basin. *Nature Communications,* 3, 834.

Ruppel, C.D., Kessler, J.D., 2016. The Interaction of Climate Change and Methane Hydrates. *Reviews of Geophysics* 55, 10.1002/2016RG000534.

Ryan, W.B., 2009. Decoding the Mediterranean salinity crisis. *Sedimentology,* 56, 95-136.

Ryan, W.B., Carbotte, S.M., Coplan, J.O., O'Hara, S., Melkonian, A. *et al.*, 2009. Global Multi-Resolution Topography synthesis. *Geochemistry, Geophysics, Geosystems,* 10, 10.1029/2008GC002332.

Saffman, P.G., 1992. Vortex dynamics. Cambridge University Press.

Sapienza, P., collaboration, N., 2005. A km 3 detector in the Mediterranean: status of NEMO. *Nuclear Physics B-Proceedings Supplements,* 145, 331-334.

Schmale, O., Leifer, I., Deimling, J.S.v., Stolle, C., Krause, S. *et al.*, 2015. Bubble transport mechanism: indications for a gas bubble-mediated inoculation of benthic methanotrophs into the water column. *Continental Shelf Research,* 103, 70-78.

Schmid, M., Lorke, A., Dinkel, C., Tanyileke, G., Wüest, A., 2004. Double-diffusive convection in Lake Nyos, Cameroon. *Deep Sea Research Part I: Oceanographic Research Papers,* 51, 1097-1111.

Skarke, A., Ruppel, C., Kodis, M., Brothers, D., Lobecker, E., 2014. Widespread methane leakage from the sea floor on the northern US Atlantic margin. *Nature Geoscience,* 7, 657-661.

Smith, A.J., Mienert, J., Bünz, S., Greinert, J., 2014. Thermogenic methane injection via bubble transport into the upper Arctic Ocean from the hydrate-charged Vestnesa Ridge, Svalbard. *Geochemistry, Geophysics, Geosystems,* 15, 1945-1959.

Socolofsky, S., Adams, E., 2002. Multi-phase plumes in uniform and stratified crossflow. *Journal of Hydraulic Research,* 40, 661-672.

Solomon, E.A., Kastner, M., MacDonald, I.R., Leifer, I., 2009. Considerable methane fluxes to the atmosphere from hydrocarbon seeps in the Gulf of Mexico. *Nature Geoscience,* 2, 561-565.

Tudino, T., Bortoluzzi, G., Aliani, S., 2014. Shallow-water gaseohydrothermal plume studies after massive eruption at Panarea, Aeolian Islands, Italy. *Journal of Marine Systems,* 131, 1-9.

Vogt, P.R., Crane, K., Sundvor, E., Max, M.D., Pfirman, S.L., 1994. Methane-generated pockmarks on young, thickly sedimented oceanic crust in the Arctic: Vestnesa ridge, Fram Strait. *Geology,* 22, 255-258.

von Deimling, J.S., Linke, P., Schmidt, M., Rehder, G., 2015. Ongoing methane discharge at well site 22/4b (North Sea) and discovery of a spiral vortex bubble plume motion. *Marine and Petroleum Geology,* 68, 718-730.

Wang, L.K., Shammas, N.K., Selke, W.A., Aulenbach, D.B., 2010. Gas dissolution, release, and bubble formation in flotation systems, Flotation Technology. Springer, pp. 49-83.

Warzinski, R.P., Lynn, R., Haljasmaa, I., Leifer, I., Shaffer, F. *et al.*, 2014. Dynamic morphology of gas hydrate on a methane bubble in water: Observations and new insights for hydrate film models. *Geophysical Research Letters,* 41, 6841-6847.

Weber, T.C., Mayer, L., Jerram, K., Beaudoin, J., Rzhanov, Y. *et al.*, 2014. Acoustic estimates of methane gas flux from the seabed in a 6000 km2 region in the Northern Gulf

of Mexico. *Geochemistry, Geophysics, Geosystems,* 15, 1911-1925.

Wilson, D.S., Leifer, I., Maillard, E., 2015. Megaplume bubble process visualization by 3D multibeam sonar mapping. *Marine and Petroleum Geology,* 68, 753-765.

Wood, W.T., Jung, W.-Y., 2008. Modeling the extent of Earth's marine methane hydrate cryosphere. p. 6-10. In: *Proceedings of the 6th International Conference on Gas Hydrates* (ICGH 2008).

Xing, J., Spiess, V., 2015. Shallow gas transport and reservoirs in the vicinity of deeply rooted mud volcanoes in the central Black Sea. *Marine Geology,* 369, 67-78.

Yamamoto, S., Alcauskas, J.B., Crozier, T.E., 1976. Solubility of methane in distilled water and seawater. *Journal of Chemical and Engineering Data* ,21, 78-80.

You, K., Kneafsey, T.J., Flemings, P.B., Polito, P., Bryant, S.L., 2015. Salinity-buffered methane hydrate formation and dissociation in gas-rich systems. *Journal of Geophysical Research: Solid Earth,* 120, 643-661.